JOURNAL OF MATERIALS SCIENCE 29 (1994) 3630–3636

Effect of hot-pressing time and post-heat treatment on the microstructure and mechanical properties of SiC-fibre-reinforced glass–ceramic composites

HYUN-HO SHIN AND ROBERT F. SPEYER
School of Materials Science and Engineering, Georgia Institute of Technology, Atlanta, GA 30332, USA

Nicalon-SiC-fibre-reinforced (35 vol%) lithium-aluminosilicate (LAS) glass–ceramic composites were fabricated by a slurry-infiltration process followed by hot pressing at 1400 °C and 10 MPa for varying soaking times. The ultimate strength and elastic modulus of the as-fabricated composites, as determined by four-point flexural tests, increased rapidly with the densification time, saturating after 30 min at 550 MPa and 130 GPa, respectively. Longer hot-pressing times caused a decrease in the elastic modulus via fibre degradation. A carbon-rich interfacial layer formed between the fibres and the matrix, the thickness of which reached a maximum of $\sim$ 400 nm after $\sim$ 30 min soaking time. The flexural strength of post-heat-treated composites in air decreased by a factor of approximately four, due to oxidation and removal of the carbon content of the interfacial layer. The silica-rich bridges left behind between the fibres and the matrix contributed to brittle fracture of the composite.

1. Introduction

Ceramic-matrix composites, developed after extensive research on polymer-matrix composites and metal-matrix composites, have used various media for the reinforcement including particles, platelets, whiskers and fibres. Fibres have been the most promising in increasing the toughness and the flaw resistance of ceramic materials. After becoming commercially available from the Nippon Carbon Company, Nicalon SiC fibres (yarn) have been used to reinforce glass or glass–ceramic matrices by slurry infiltration of the yarn, followed by hot pressing [1, 2], or to reinforce some non-oxide matrices formed by chemical vapour infiltration (CVI) [3, 4]. The slurry-infiltration method has the benefit of straightforward fabrication. However, the preforms are limited to simple shapes due to the geometric restrictions of hot pressing. The CVI method is more appropriate for complex preforms, but it is a relatively multifarious, slow, and expensive process, resulting in a more porous product than in methods involving slurry infiltration.

Nicalon SiC fibres [5] with a high elastic modulus (176 $\sim$ 196 GPa) and strength (2.45 to 2.94 GPa) can greatly reinforce glasses [6] of lower elastic modulus (50–90 GPa) and strength ($\sim$ 100 MPa). The coefficient of linear thermal expansion of the fibres ($4.7 \times 10^{-6}\,^{\circ}C^{-1}$) is higher than that of the matrix ($\sim 1.5 \times 10^{-6}\,^{\circ}C^{-1}$ for LAS glass–ceramic [6]). This causes a compressive stress to form in the matrix in the direction of the fibre axis during cooling after hot pressing. This, in turn, results in a higher tensile strength for the composite, since a compensating force for internal compressive forces is required before true elongation occurs in the matrix under tensile loading.

The low viscosity of the glass/glass–ceramic matrix during hot pressing avoids mechanical damage to the fibres during the physical densification of the composites. A carbon-rich interfacial layer is formed during hot pressing by reaction between the fibre and the matrix [2, 7]. This interfacial layer, which is of limited bond strength, promotes crack deflection, multiple matrix cracking, fibre debonding and fibre pull-out [8, 9, 10, 11] during fracture. These mechanisms result in a flaw-tolerable (notch-independent fracture) composite with a markedly improved fracture toughness over the unreinforced matrix. At the same time, the interfacial bonding is strong enough for appreciable load transfer to the fibres. Such interfacial-layer formation is more enhanced in matrices containing a liquid phase during hot pressing [12]. Such liquid phases provide soluble gas for reaction with the SiC fibres. The presence of such liquid phases also acts to prevent fibre damage during hot pressing.

In the conventional slurry-infiltration fabrication process [1, 13], the fibres are first heat treated or treated chemically to remove the protective organic coating provided by the manufacturer, and then they are dipped into a slurry containing a ground-glass powder and a binder solution. The slurry-containing fibres are then wound on teflon-coated drums and prepared into tapes. These tapes are dried, sectioned and laid into shapes suitable for hot pressing. They are then heated in air to burn off the binder, and then hot pressed in graphite dies without an externally

0022–2461

imposed atmosphere. The variables considered in the optimization of the fabrication parameters are those involved in either the slurry infiltration (slurry composition to control viscosity, winding speed, fibre tension) or in the hot pressing (time, temperature and pressure). The slurry-infiltration parameters were adjusted to control the amount of slurry infiltrated into the fibres, and ultimately to control the volume percentage of fibres in the final composite.

In a modified slurry-infiltration method described in the next section, the fibre volume percentage is more directly controlled and hence the hot-pressing parameters are the only variables affecting the resultant composite properties. The thickness of the carbon-rich interfacial layer is known to vary with the hot-pressing conditions [14]. At issue, as one intended focus of this study, is a correlation of the thickness of the interfacial layer (controlled by the soaking time) to the mechanical behaviour of the composite.

When nucleating agents (Nb_2O_5, Ta_2O_5, TiO_2, etc.) were used to devitrify the LAS matrix an additional carbide phase (NbC, TaC, TiC, etc.) was formed between the carbon-rich interfacial layer and the matrix [15]. However, in order to minimize the variables in the correlation of the interfacial-layer thickness with the mechanical properties, additional carbide phases were avoided. Hence, no nucleating agents were used in this study.

2. Experimental procedure

A material with the composition $Li_2O \cdot Al_2O_3 \cdot 4SiO_2$ was selected for the matrix. The crystalline form of this composition (β-spodumene) formed the most refractory compound within the solid solution [16]. Li_2CO_3 was used for the Li_2O constituent in the glass batch. The batch was melted in a platinum crucible at 1650 °C for 6 h using a $MoSi_2$-heating-element furnace. The glass melt was then quenched, crushed, and ball milled using a zirconia medium, to produce a particle size distribution entirely less than 10 μm in diameter (as determined by scanning electron microscopy (SEM)). The glass slurry was prepared by mixing 35 wt % of glass powder with 65 wt % of a poly vinyl alcohol (PVA)/water solution using a magnetic stirrer in a closed container.

In a modified slurry-infiltration process, the SiC fibres (10 ~ 20 μm in diameter) were cut into 6 cm lengths and then heat treated in air at 350 °C for 20 min to remove a protective organic coating provided by the manufacturer. The fibres were then unidirectionally aligned in a rectangular box ($6 \times 6 \times 2$ cm^3) made of graphite foil. Then, an appropriate amount of the glass-containing slurry was poured into the box. This ensemble was dried in an air-circulating oven at 120 °C. Binder removal was accomplished by heat treating the graphite-foil box containing the green body at 600 °C for 20 min in air. Hot pressing was performed in graphite dies at 1400 °C for 10, 20, 30, 60 and 120 min (at 10 MPa) in an induction-heated instrument. Pressure was applied during heating, starting at 1350 °C, and removed at the same temperature during cooling. The resultant composites contained an average of 35 vol % of the fibre (determined by a SEM image analysis of the composite cross-section).

For measurement of the interfacial-layer thickness by SEM (Hitachi Ltd Model S800), as-fabricated composites were cut perpendicularly to the fibre direction, ground and polished using a 0.3 μm alumina polishing media, and a conductive Au coating was then applied. At least 15 representative SEM photomicrographs of fibres in the matrix were used for each specimen. The thicknesses of the interfacial layers were measured from the micrographs. The error bars for the thickness results represent the standard deviation from the mean thickness. SEM energy dispersive spectroscopy (Kevex, San Carlos, CA, USA) was used to determine chemical constituents. A series of spectra were taken, extending radially from the fibre through the interface and into the matrix, to ensure that excitation volume effects did not give a false impression of the local chemistry. Transmission electron microscopy (TEM, JEOL model 2000X, Tokyo, Japan) samples were cut into 3 mm discs along the fibre direction, thinned mechanically to 120 μm, dimpled to 40 μm, and then Ar-ion milled to electron transparency using a liquid-nitrogen cold stage. The density of the as-fabricated composites was measured using the Archimedes principle with an analytical balance with a precision of 0.01 mg.

For mechanical characterization, the composites were cut and polished into blocks ~ $1.7 \times 3 \times 60$ mm^3, with the longest dimension along the fibre direction. At least 5 ~ 6 composites were tested after fabrication under each thermal schedule. The flexural properties (ultimate strength and elastic modulus) were measured using a four-point flexural test (Instron, Model 8562, Canton MA, USA) with a 1/3 span (inner span, 15 mm; outer span, 45 mm) and a loading rate of 0.5 mm min^{-1}. Initial three-point tests were made with a 40 mm span at the same loading rate. Data scatter for the flexural composite strength and the elastic modulus is indicated in subsequent figures (Figs 7 and 9) by error bars, representing the standard deviation about the mean. Apparent elastic moduli were determined from initial tangent lines to cross-head-displacement-versus-load curves. The compliance of the Instron machine was not accounted for. For a load span of one-third of the support span and a highly anisotropic composite [17],

$$E_H = \frac{0.21 L^3 m}{b d^3}$$

where E_H is the modulus of elasticity in bending (N m^{-3}), L is the support span (m), b is the width of the beam (m), d is the depth of the beam (m) and m is the slope of the tangent to the initial straight-line portion of the load–deflection curve (N m^{-1}).

3. Results

X-ray diffraction (XRD) results showed that after hot pressing at 1400 °C for 20 min, the LAS matrix devitrified to form a β-spodumene solid solution. Differences in the XRD peak heights, which indicate changes in

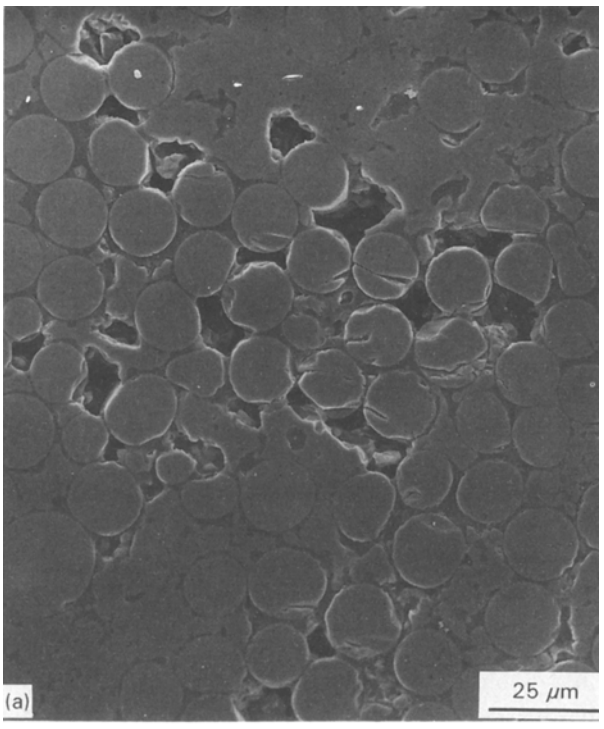

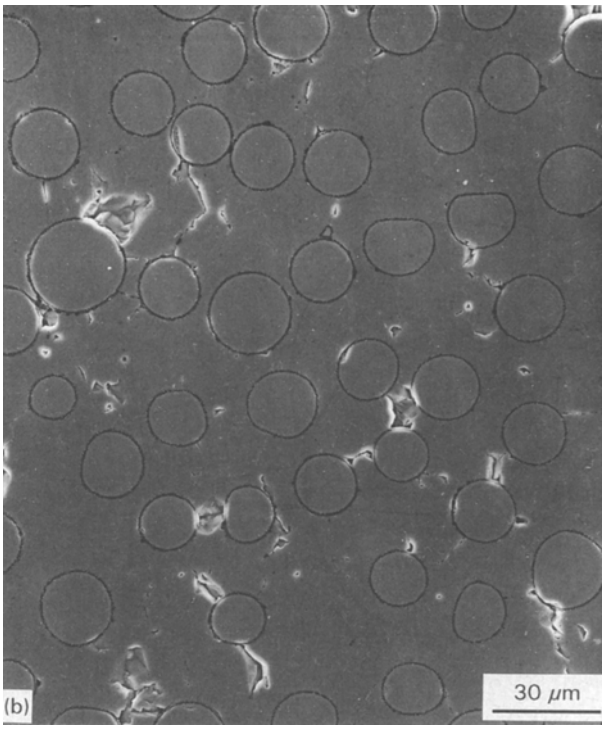

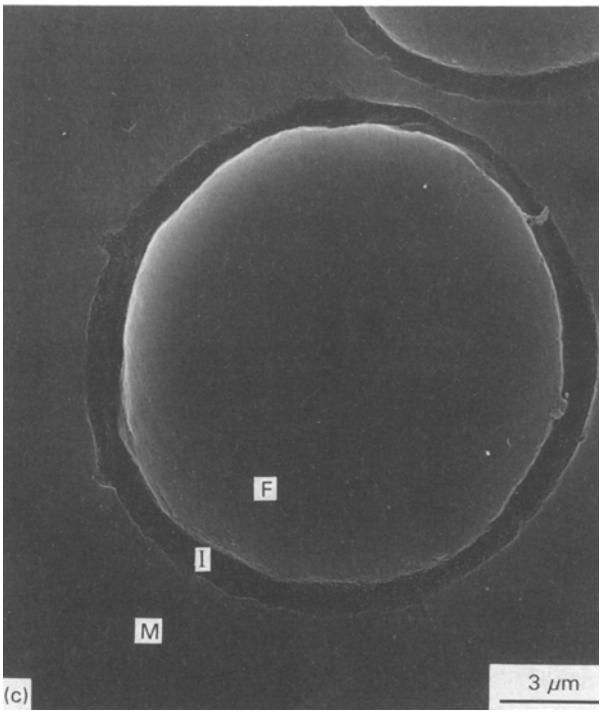

Figure 1 SEM (secondary electron) micrographs of a composite cross-section after hot pressing, showing the distribution of fibres within the glass–ceramic matrix: (a) 10 min at 1400 °C; (b) 30 min at 1400 °C (matrix cracking occurred during SEM-sample preparation, and (c) a higher magnification micrograph of Fig. 1b showing a well-developed interfacial layer between the fibre and the matrix (F, fibre, I, interfacial layer, and M, matrix).

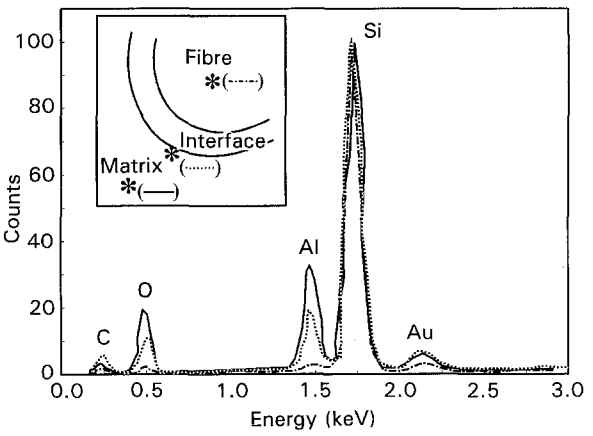

Figure 2 SEM energy dispersive spectroscopy (EDS) of the locations marked in the inset sketch. All the peak intensities were normalized to the intensity of silicon so that the silicon-to-aluminium ratio could be easily compared. EDS spectra of the interface were taken in partial overlap with the matrix to ensure that the excitation volume did not reach the fibre.

the fraction devitrified, were not apparent between patterns for the composites hot pressed for varying soaking periods. TEM observation of the matrices did indicate that a greater fraction crystallized in the matrix after 120 min than after 20 min. β-spodumene crystal sizes were of the order of 2–8 μm in diameter.

Figs 1a and 1b are typical microstructures of composite cross-sections. A higher percentage matrix porosity was apparent as the hot-pressing time decreased. Fig. 1c shows a well-developed interfacial layer between the fibre and the matrix. As shown in Fig. 2, the carbon-rich interface had a higher silicon to aluminium ratio than that of the matrix. The gold peak was from the conductive coating deposited on the specimen.

To determine the hot-pressing temperature at which the hot-pressing times were to be varied, composites were hot-pressed at varying temperatures for a constant 20 min soaking period. Considering the melting point of the β-spodumene solid solution (1425 °C), the hot-pressing temperatures were varied from 1350 to 1400 °C. The flexural-strength values of composites fabricated in this temperature range are shown in Fig. 3. Based on these results, a hot-pressing temperature of 1400 °C was selected for the study of the effects of the hot-pressing time.

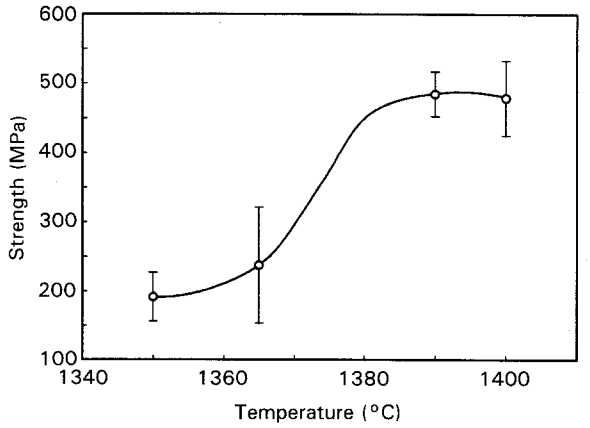

Figure 3 The effect of the hot-pressing temperature on the flexural strength of composites after a soaking time of 20 min. The data represent calculations based on both three-point- and four-point-bending tests.

Fig. 4 shows the effect of the hot-pressing time on the appearance of the interfacial layer. For short hot-pressing times (for example 20 min), dark and light textures within the interfacial layer imply phase-separated amorphous regions of different compositions. After longer times, the darker phase appears to have segregated to form a line within the carbon-rich interfacial layer.

From measurements on micrographs like Fig. 1b, the variation of the interfacial-layer thickness with the hot-pressing time was determined (Fig. 5). The thickness of the layer rapidly increased over short soaking periods and then it reached a maximum after $\sim$ 30 min of soaking time. The density of the composites increased with the hot-pressing time at 1400 °C, as shown in Fig. 6. Using the measured glass ($Li_2O \cdot Al_2O_3 \cdot 4SiO_2$) density of 2400 kg m^{-3} and a reported fibre density of 2600 kg m^{-3} [18], a fibre volume fraction of 0.35, and neglecting the contribution of the interfacial layer, the theoretical density of the composites predicted by the rule of mixtures is 24700 kg m^{-3}.

The effect of the hot-pressing time on the room-temperature ultimate strength of the composites is shown in Fig. 7a. The ultimate strength and elastic modulus (Fig. 7b) values reached a maximum after a hot-pressing time of $\sim$ 30 min. In all cases, non-brittle fracture was observed. Fig. 8 shows the path of a crack, which only propagated after appreciable fibre debonding at the interface between the matrix and the carbon-rich layer.

The variation in the flexural properties (strength and elastic modulus), exposed to secondary heat treatments at 1000 °C for 0.5 h in air, with the original hot-pressing time are shown in Fig. 9. Both properties initially increased with the hot-pressing soaking period, remaining more or less constant after $\sim$ 30 min soaking time. Fig. 10 shows the interfacial microstructure of a fracture surface of the composite after secondary heat treatment. As can be seen, air-gaps replaced much of the carbon-rich interfacial layer. The interfacial chemistry of the bridges formed between the fibre and the matrix, as compared to the chemistry of the matrix, is shown in Fig. 11. A significant decrease in the aluminium-to-silicon ratio in the bridging phase, compared to the matrix, is apparent.

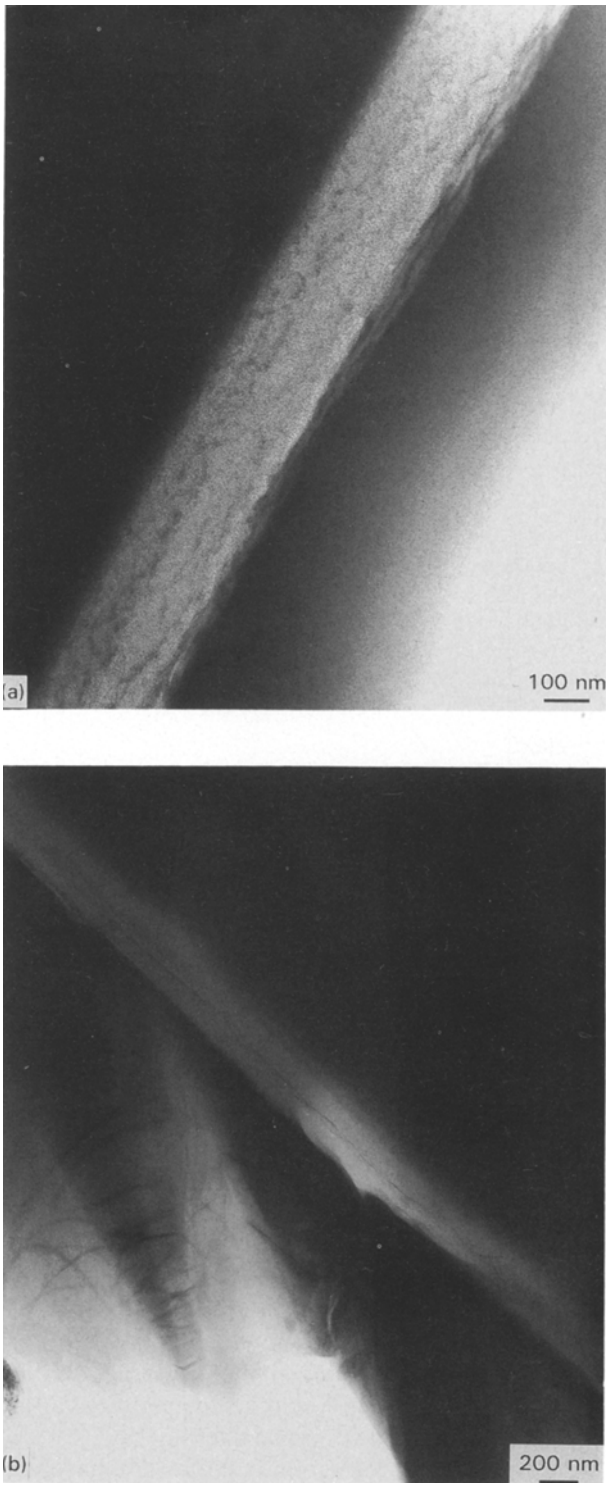

Figure 4 TEM micrographs of the carbon-rich interfacial layer after hot pressing at 1400 °C for: (a) 20 min, and (b) 120 min.

4. Discussion

The LAS matrix composition used ($Li_2O \cdot Al_2O_3 \cdot 4SiO_2$) was adequately unstable so that devitrification occurred during heating without the use of nucleation agents. A more silica-rich composition used in a previous work, $Li_2O \cdot Al_2O_3 \cdot 6SiO_2$, also without nucleating agents, did not devitrify [19] under heat treatment. The relatively lower silica content in the

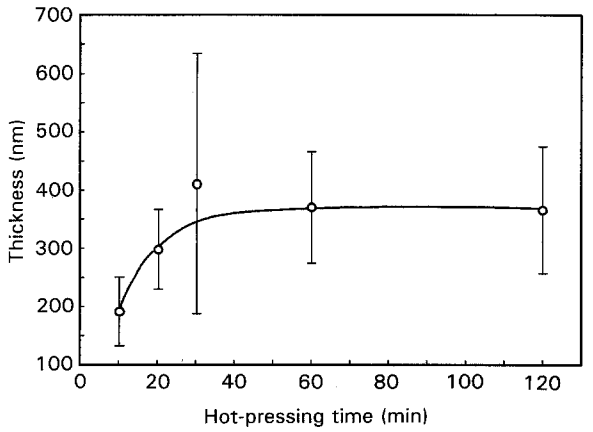

Figure 5 The effect of the hot-pressing time at 1400 °C on the thickness of the interfacial layer.

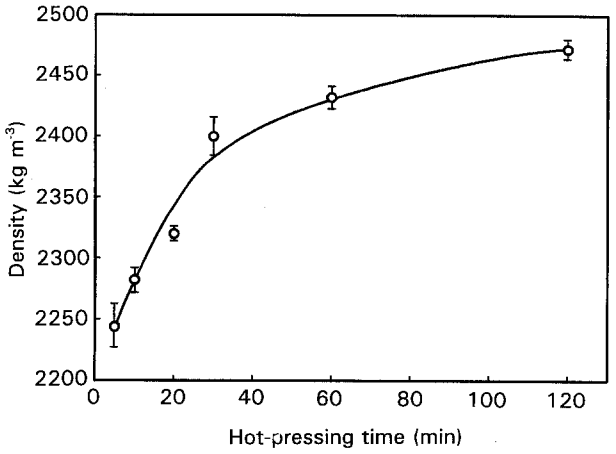

Figure 6 The effect of the hot-pressing time at 1400 °C on the density of the as-fabricated composites. The error bars represent the standard deviation in the density measurements of the same specimen (two measurements per hot-pressing time period).

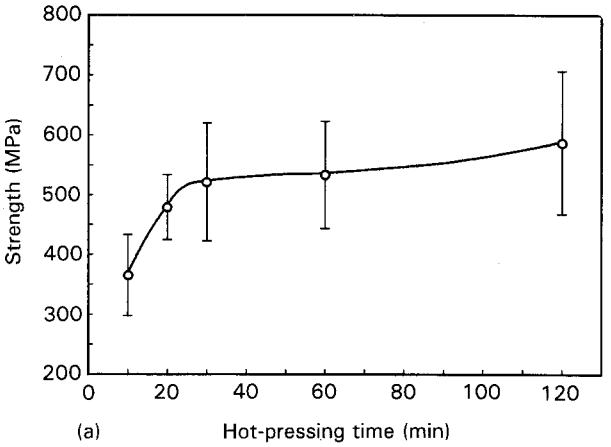

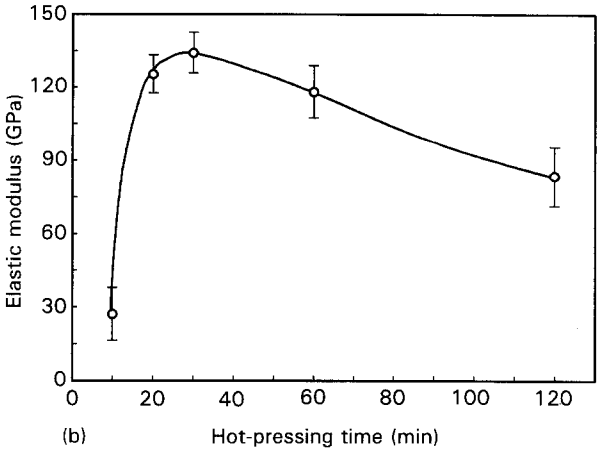

Figure 7 The effect of the hot-pressing time at 1400 °C on: (a) the ultimate strength in four-point flexural tests, and (b) the elastic modulus based on four-point flexural tests.

glass composition studied is expected to have resulted in a less-stable glass.

Higher-temperature hot pressing facilitated stronger composites. This resulted from the increased fluidity of the glassy phase during hot pressing, which in turn permitted more rapid pore elimination. Although 1400 °C was selected for the hot-pressing soaking temperature, from Fig. 3, soaking temperatures as low as 1380 °C would have served the same ends.

Interfacial-layer formation is expected to have started during heating to the soaking temperature. The increase in the interfacial-layer thickness appeared to reach a terminal value after ~ 30 min of soaking (Fig. 5). The dark interface in the SEM micrograph in Fig. 1b indicates that the interface consisted of elements which are light relative to the matrix and fibres. Consistent with this, the EDS results (Fig. 2) indicate that this region contains carbon. The presence of aluminium peaks in the interface, even near the SiC fibre (not shown), implies that the glassy phase from the matrix was somewhat soluble in the interfacial layer. However, the higher silicon-to-aluminium ratio in the interfacial layer (relative to the matrix) indicates that the interface is rich in silicon. Based on this, the interfacial layer can be considered to have formed in a reaction between the SiC fibres and soluble carbon

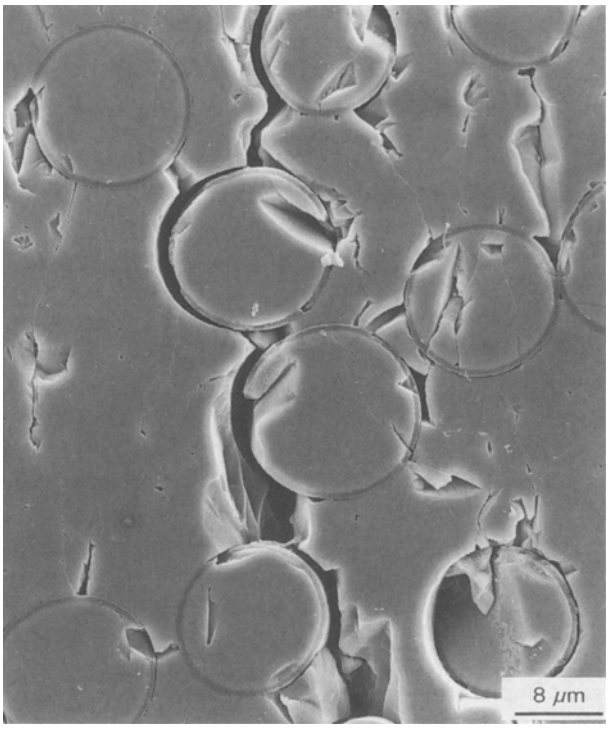

Figure 8 Crack propagation along matrix–fibre interfaces of a polished section of a specimen fractured under four-point bending.

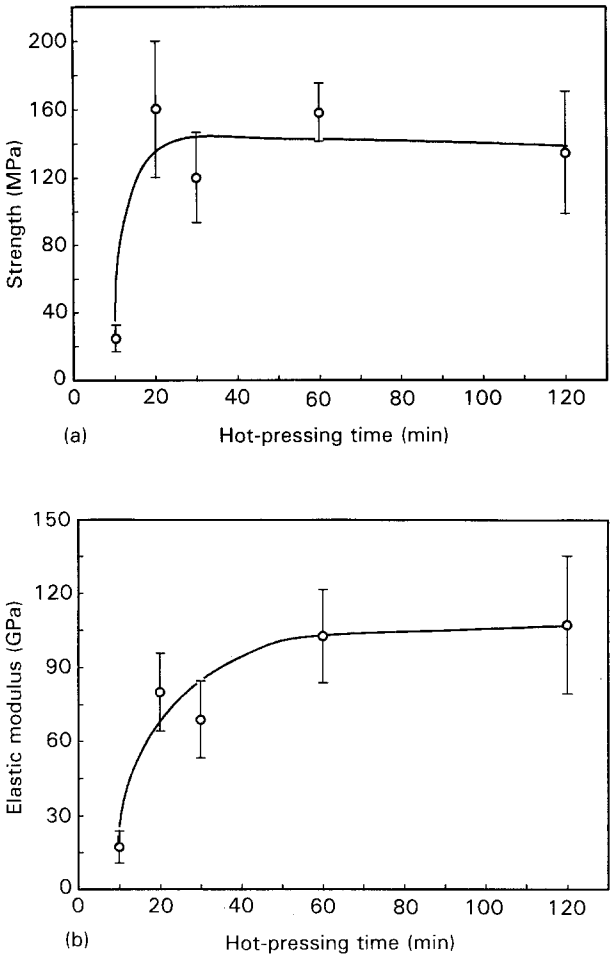

Figure 9 The effect of the hot-pressing time at 1400 °C on: (a) the ultimate strength, and (b) the elastic modulus. All the composites were exposed to secondary heat treatments at 1000 °C for 30 min in air.

monoxide from the fluid portions of the matrix, with the product being carbon and amorphous silica. Carbon monoxide would be provided by the hot-press atmosphere as a reaction product of oxy and the graphite dies. Dark (silica) and light (carbon) amorphous phases appear to segregate with extended hot-pressing times (Fig. 4).

The increases in the flexural strength and the elastic modulus cannot be directly linked to increases in the interfacial-layer thickness. Appreciable densification occurred simultaneously with interfacial-layer coarsening. The measured increase in the composite density (Fig. 6) would result from glass-particle consolidation and devitrification to a β-spodumene solid solution. The elimination of the porosity, and its associated stress concentrations, is undoubtedly the dominant cause of the increase in the measured ultimate strength. It is unfortunately not possible, therefore to establish the effect of the interfacial-layer thickness on the mechanical properties by varying the hot-pressing parameters. However, as is apparent in Fig. 8, debonding occurred at the contact point between the carbon-rich interfacial layer and the matrix, rather than within the interfacial layer or the contact between the interface and the fibre. This implies that the fracture behaviour is independent of the interfacial-layer thickness for a well-established interfacial layer.

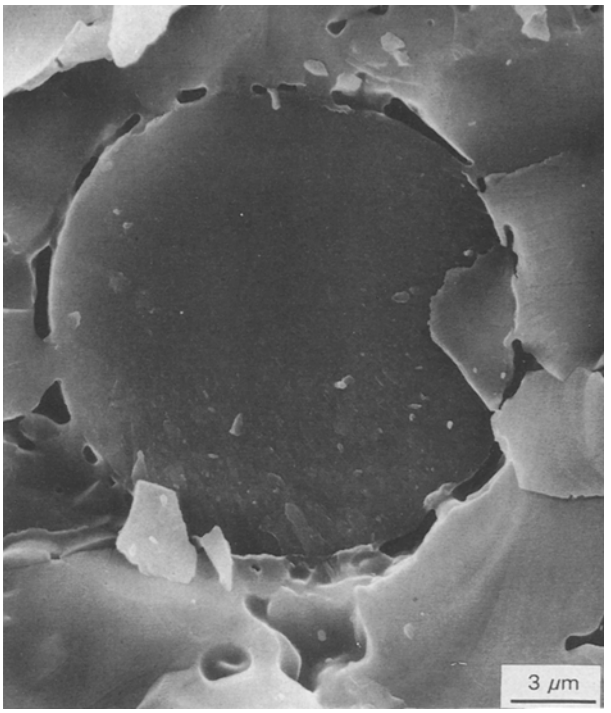

Figure 10 The interfacial microstructure of the hot-pressed composite after secondary heat treatments at 1000 °C for 30 min in air.

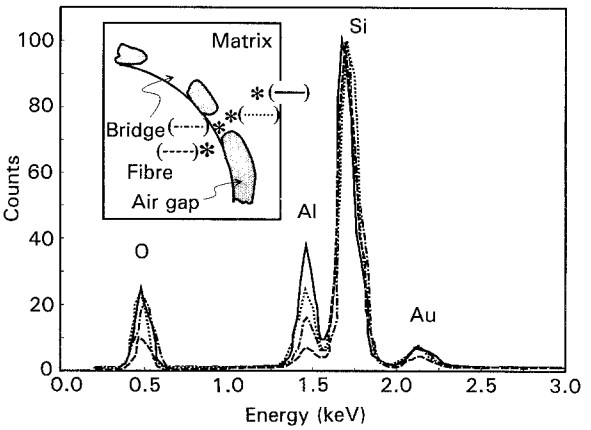

Figure 11 Energy dispersive spectroscopy of a fracture surface of a composite post-heat-treated in air at 1000 °C for 30 min. All the peaks were normalized to that of silicon. A decreased aluminium-to-silicon ratio was observed moving from the matrix through the bridging region and into the fibre. The asterisks in the inset sketch indicate positions in which the spectra were taken.

The lower flexural strength values obtained in Fig. 7a (compared to other work [20]) may originate from the way in which the displacement was measured, or it may have been fostered by the lack of nucleating agents (for example Nb_2O_5 and Ta_2O_5) in the matrix composition. The β-spodumene-solid-solution crystal sizes of 2–8 μm which formed in the composites without nucleating agents are vastly larger than those with nucleating agents (for example, ~ 10 nm). The internal stresses developed from anisotropic contraction during cooling in the hot press would have diminished the load-bearing capacity of the matrix. The additional carbide phase (for example, NbC or TaC), which forms at the interface as a result of nucleation-agent addition, has also been reported to increase the composite strength [20, 21].

The elastic modulus as determined by flexural tests (Fig. 7b) initially sharply increased with the hot-pressing time, since the more densified matrix was better able to contribute mechanical resistance to the applied load. For hot-pressing times exceeding the 30 min soaking period, the elastic modulus decreased. The degradation of SiC-fibre properties when exposed to temperatures in excess of 1000 °C has been well-established [22]. In the absence of an oxidizing atmosphere, the fibres degrade by SiC grain growth and CO evolution (from constituents within the fibre). The resultant fissures and porosity formed within the fibre would reduce the load-bearing cross-sectional area. The decrease in the measured elastic modulus of composites hot pressed for long times can therefore be interpreted to be a result of decreasing fibre stiffness.

Post-heat-treatment did not appreciably effect the elastic modulus of the composite, but it markedly decreased the measured ultimate strength. The stresses at fracture dropped to approximately one fourth of the ultimate strength of the composites without post-heat-treatment. At 1000 °C, oxygen penetration into the composite from the atmosphere was appreciable. During post-heat-treatment in air, the carbon-rich interfacial layer was removed by oxidation ($C_{(s)} + O_{2(g)} = CO_{2(g)}$ or $C_{(s)} + \frac{1}{2}O_{2(g)} = CO_{(g)}$), leaving an amorphous silica-rich bridging phase behind at the interface (Figs 10 and 11). The enhanced presence of silica provides further corroboration for the mechanism of carbon-rich interfacial formation: $SiC + 2CO = 3C + SiO_2$. Additional silica at the interface may have been formed by oxidation of the surface of the silicon-carbide fibre. However, there would be no propensity for silica formed in this fashion to develop discontinuous bridges between the fibres and the matrix.

The observed decrease in the flexural strength coincides with a reversion to a brittle fracture mechanism wherein cracks propagated from the matrix directly through the fibres. This was caused by the strong bonding between the fibres and the matrix from the fused silica-rich interface. Stress concentrations at the silica-rich bridges initiated extension of critical flaws at lower applied stresses. The only minor decrease in the flexural elastic modulus, which is dominated by the elastic modulus of the fibre, indicates that post-heat-treatment continued to only slightly degrade the stiffness of the fibres. The silica layer which formed around the fibre via oxidation may prevent volatilization of species from within, preserving its integrity [22].

5. Conclusion

The increase in the elastic modulus and the ultimate strength of the composite with soaking time up to ~ 30 min was accompanied by interfacial-layer coarsening as well as by matrix densification. Preferential debonding at the contact point between the *C-rich* interphase and the matrix implied that fracture behaviour was independent of interphase thickness for a well established interphase. A slight decrease in the elastic modulus for longer times is attributed to fibre degradation. Post-heat-treatment in air (1000 °C for 20 min) showed a dramatic removal of the carbon-rich layer by oxidation to CO or CO_2, leaving behind silica-rich bridges between the fibres and the matrix. This resulted in brittle fracture of the composite and a fourfold reduction in the ultimate strength.

References

1. J. J. BRENNAN and P. M. PREWO, *J. Mater. Sci.* **17** (1987) 2371–83.
2. R. F. COOPER and K. CHYUNG, *ibid.* **22** (1987) 3148–60.
3. R. D. VELTRI and F. S. GALASSO, *J. Amer. Ceram. Soc.* **73** (1990) 2137–40.
4. D. P. STINTON, A. J. CAPUTO and R. A. LOWDEN, *Amer. Ceram. Soc. Bull.* **65** (1986) 347–50.
5. T. ISHIKAWA and H. TERANISHI, *New Mater. New Proc.* **1** (1981) 36–41.
6. R. A. HABER and R. M. ANDERSON, "Ceramics and glasses, engineered materials handbook", Vol. 4, edited by J. Schneider Jr, (American Society for Metals, Metals Park, OH, 1991).
7. P. M. BENSON, K. E. SPEAR and C. G. PANTANO, *Ceram. Engng. Sci. Proc.* **9** (1988) 663–70.
8. A. G. EVANS, M. Y. HE and J. W. HUTCHISON, *J. Amer. Ceram. Soc.* **72** (1989) 2300–303.
9. M. D. THOULESS, O. SBAIZERO, L. SIGL and A. G. EVANS, *ibid.* **72** (1989) 525–32.
10. J. AVESTON, G. A. COOPER and A. KELLY, "Single and multiple fracture", in "Properties of fiber composite", National Physical Laboratory Conference Proceedings (IPC Science and Technology Press, Guildford, England, 1971).
11. D. B. MARSHALL and A. G. EVANS, *J. Amer. Ceram. Soc.* **68** (1985) 225–31.
12. H. H. SHIN, Y. BERTA, C. PARK and R. F. SPEYER, Proceedings of the 50th Annual Meeting of the Electron Microscopy Society of America, edited by G. W. Bailey, J. Bentley and J. A. Small (San Francisco Press, San Francisco, 1992).
13. R. CHAIM and A. H. HEUER, *Adv. Ceram. Mater.* **2** (1987) 154–58.
14. J. HOMENY, J. R. VAN VALZAH and M. A. KELLY, *J. Amer. Ceram. Soc.* **73** (1990) 2054–59.
15. J. Y. HSU and R. F. SPEYER, *J. Mater. Sci.* **27** (1992) 374–80.
16. R. ROY, D. M. ROY and E. F. OSBORN, *J. Amer. Ceram. Soc.* **33** (1950) 152–159.
17. Standard Test Methods for Flexural Properties of Unreinforced and Reinforced Plastics and Electrical Insulating Materials: D790-91, "Annual book of ASTM standards", (American Society for Testing and Materials, Philadelphia, 1991).
18. K. K. CHAWLA, "Composite materials, sicence and engineering" (Springer-Verlag, New York, 1987) p. 46.
19. J. Y. HSU and R. F. SPEYER, *J. Amer. Ceram. Soc.* **74** (1991) 395–99.
20. K. M. PREWO, J. J. BRENNAN and G. K. LAYDEN, *Amer. Ceram. Soc. Bull.* **65** (1986) 305–13, 322.
21. J. Y. HSU and R. F. SPEYER, *J. Mater. Sci.* **27** (1992) 381–90.
22. T. MAH, N. L. HECHT, D. E. McCULLUM, J. R. HOENIGMAN, H. M. KIM, A. P. KATZ and H. A. LIPSITT, *ibid.* **19** (1984) 1191–1201.

Received 11 November 1993
and accepted 3 February 1994